Robotica (2006) volume 24, pp. 499–511. © 2006 Cambridge University Press
doi:10.1017/S0263574705002511 Printed in the United Kingdom

Techniques for vibration control of a flexible robot manipulator

Z. Mohamed*, A. K. Chee*, A. W. I. Mohd Hashim*, M. O. Tokhi†, S. H. M. Amin* and R. Mamat*

(Received in Final Form: October 25, 2005. First published online: January 23, 2006)

SUMMARY

This paper presents investigations into the applications and performance of positive and negative input shapers in command shaping techniques for the vibration control of a flexible robot manipulator. A constrained planar single-link flexible manipulator is considered and the dynamic model of the system is derived using the finite element method. An unshaped bang-bang torque input is used to determine the characteristic parameters of the system for design and evaluation of the input shaping control techniques. The positive and specified amplitude negative input shapers are designed based on the properties of the system. Simulation results of the response of the manipulator to the shaped inputs are presented in the time and frequency domains. Performances of the shapers are examined in terms of level of vibration reduction, time response specifications and robustness to parameters uncertainty. The effects of derivative order of the input shaper on the performance of the system are investigated. Finally, a comparative assessment of the impact amplitude polarities of the input shapers on the system performance is presented and discussed.

KEYWORDS: Flexible manipulator; Input shaping; Simulation; Vibration control.

I. INTRODUCTION

Manipulator arms have traditionally been designed to have rigid links to ensure stable and reliable control. Minimum vibration and good positional accuracy are achieved by maximising the stiffness of the system. To design a 'stiff' system, normally heavy material is used. As a consequence, the rigid-link manipulators are usually large and massive with respect to the operating payload. The drawbacks of these large and massive robot manipulators are the limitation of the operation speed, the increase of the size of actuators and higher energy consumption. In contrast, flexible robot manipulators exhibit several advantages over the rigid link manipulators as they require less material, are lighter in weight, have higher manipulation speed, lower power consumption, require smaller actuators, are more manoeuvrable and transportable, have less overall cost and higher payload to robot weight ratio.[1]

However, the control of flexible manipulators to maintain accurate positioning is a challenging problem. A flexible manipulator is a distributed parameter system and has infinite modes of vibration. Moreover, the dynamics are highly non-linear and complex. Problems arise due to precise positioning requirements, system flexibility leading to vibration, the difficulty in obtaining accurate model of the system and non-minimum phase characteristics of the system.[2] To attain end-point positional accuracy, a control mechanism that accounts for both the rigid body and flexural motions of the system is required. If the advantages associated with lightness are not to be sacrificed, precise models and efficient control strategies for flexible manipulators have to be developed.

The requirement of precise position control of flexible manipulators implies that vibration of the system should be zero or near zero. Over the years, investigations have been carried out to devise efficient approaches to reduce the vibration of flexible manipulators. The considered vibration control schemes can be divided into two main categories: feed-forward control and feedback control techniques. Feed-forward techniques for vibration suppression involve developing the control input through consideration of the physical and vibrational properties of the system, so that system vibrations at dominant response modes are reduced. This method does not require additional sensors or actuators and does not account for changes in the system once the input is developed. On the other hand, feedback-control techniques use measurement and estimations of the system states to reduce vibration. Feedback controllers can be designed to be robust to parameter uncertainty. For flexible manipulators, feed-forward and feedback control techniques are used for vibration suppression and end-point position control respectively. An acceptable system performance without vibration that accounts for system changes can be achieved by developing a hybrid controller consisting of both control techniques. Thus, with a properly designed feed-forward controller, the complexity of the required feedback controller can be reduced.

A number of techniques have been proposed as feed-forward control strategies for control of vibration. Swigert[3] has derived a shaped torque that minimises vibration and the effect of parameter variations that affect the modal frequencies. However, the forcing function is not time-optimal. Several researchers have studied the application of computed torque techniques for control of flexible manipulators.[4] However, these techniques suffers from

* Faculty of Electrical Engineering, Universiti Teknologi Malaysia, 81310 UTM, Johor (Malaysia).
† Department of Automatic Control and Systems Engineering, The University of Sheffield (UK).
Corresponding author. Dr. Z. Mohamed. E-mail: zahar@fke.utm.my

several problems.[5] These are due to inaccuracy of a model, selection of poor trajectory to guarantee that the system can follow it, sensitivity to variations in system parameters and response time penalties for a causal input.

Bang-bang control involves the utilisation of single and multiple-switch bang-bang control functions,[6] which require accurate selection of switching time(s), depending on the dynamic model of the system. Minor modelling errors could cause switching errors and result in a substantial increase in the vibrations. Meckl and Seering[7] have examined the construction of input functions from either ramped sinusoids or versine functions. The resulting input which is given to the system approaches the rectangular shape, but does not significantly excite the resonances. The method has subsequently been tested on a cartesian robot, achieving considerable vibration reduction.

Another method for feed-forward motion-induced vibration control is the command shaping technique. A significant amount of work on shaped command input based on filtering techniques has been reported. In this approach, a shaped torque input is developed on the basis of extracting the input energy around the natural frequencies of the system, so that the vibration of the flexible manipulator during and after a movement is reduced. Various filtering techniques have been employed. These include low-pass filters, band-stop filters and notch filters.[8,9] It has been shown that better performance in the reduction of level of vibration of the system is achieved using low-pass filters.

Singer and co-workers have proposed an input shaping strategy, which is currently receiving considerable attention in vibration control.[5,8,10] Since its introduction, the method has been investigated and extended. Using this method, a response without vibration can be achieved, however, with a slight time delay approximately equal to the length of the impulse sequence. With more impulses, the system becomes more robust to flexible mode parameter changes, but this will result in longer delay in the system response. Recently, an experimental study on the performance of the input shaping technique in reducing vibration of a very flexible manipulator system has been reported.[11]

To reduce the delay in the system response, negative amplitude input shapers have been introduced and investigated in vibration control. By allowing the shaper to contain negative impulses, the shaper duration can be shortened, while satisfying the same robustness constraint. Rappole et al.[12] have studied the development of time-optimal negative input shaper that requires the numerical solution of a set of simultaneous transcendental equations. Alternatively, a look-up method that generates time-optimal negative input shapers without solving a set of complicated equations has been reported.[13] In this work, the solution for the problems of over-currenting and high mode excitation that may occur with negative shapers has also been discussed. A significant number of negative shapers for vibration control have also been proposed. These include negative unity-magnitude (UM) shaper, specified-negative-amplitude (SNA) shaper, negative zero-vibration (ZV) shaper, negative zero-vibration-derivative (ZVD) shaper and negative zero-vibration-derivative-derivative (ZVDD) shaper.[14,15]

This paper presents investigations into the application and performance of input shaping control schemes with positive and SNA input shapers for vibration control of a single-link flexible manipulator. Moreover, this paper provides a comparative assessment of the performance of these schemes. The results of this work will be helpful in designing efficient algorithms for vibration control of various systems. In this work, input shaping with positive input shapers (ZV and ZVDD) and SNA input shapers (ZV and ZVDD) are considered. The dynamic model describing the motion of the flexible manipulator is derived using the finite element method. Simulation exercises are performed within the flexible manipulator simulation environment. Initially, to obtain the characteristic parameters of the system, the flexible manipulator is excited with a single-switch bang-bang torque input. Then the input shapers are designed based on the properties of the manipulator and used for pre-processing the input, so that no energy is fed into the system at the natural frequencies. Performances of the developed controllers are assessed in terms of level of vibration reduction, time response specifications and robustness to errors in vibration frequency. In this case, the robustness of the control schemes is assessed with up to 30% error tolerance in vibration frequencies. Simulation results in time and frequency domains of the response of the flexible manipulator to the unshaped input and shaped inputs with positive and SNA input shapers are presented. Moreover, a comparative assessment of the effectiveness of the positive and negative input shapers in suppressing vibration of the flexible manipulator is discussed.

II. THE FLEXIBLE MANIPULATOR SYSTEM

The single-link flexible manipulator system considered in this work is shown in Figure 1, where X_oOY_o and XOY represent the stationary and moving coordinate frames respectively, τ represents the applied torque at the hub. E, I, ρ, A, I_h and m_p represent the Young modulus, area moment of inertia, mass density per unit volume, cross-sectional area, hub inertia and payload mass of the manipulator respectively. In this work, the motion of the manipulator is confined to X_oOY_o plane. Transverse shear and rotary inertia effects are

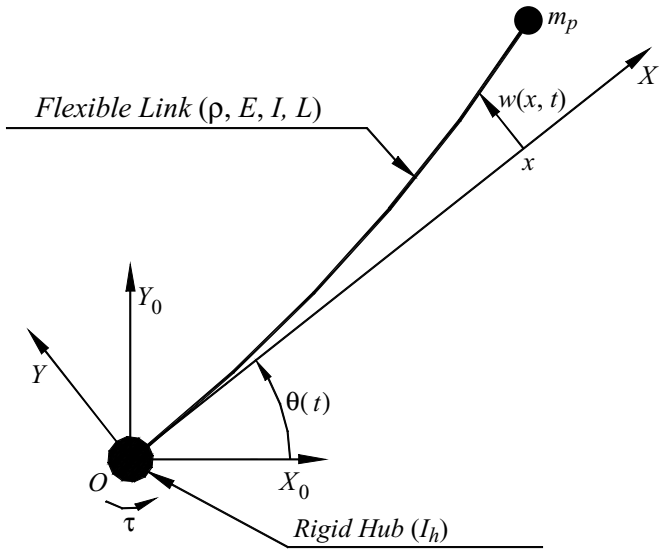

Fig. 1. Description of the flexible manipulator system.

https://doi.org/10.1017/S0263574705002511 Published online by Cambridge University Press

neglected, since the manipulator is long and slender. Thus, the Bernoulli-Euler beam theory is allowed to be used to model the elastic behaviour of the manipulator. The manipulator is assumed to be stiff in vertical bending and torsion, allowing it to vibrate dominantly in the horizontal direction and thus, the gravity effects are neglected. Moreover, the manipulator is considered to has a constant cross-section and uniform material properties throughout. In this study, an aluminium type flexible manipulator of dimensions $900 \times 19.008 \times 3.2004\,\text{mm}^3$, $E = 7 \times 10^9\,\text{N/m}^2$, $I = 5.1924 \times 10^{11}\,\text{m}^4$, $\rho = 2710\,\text{kg/m}^3$ and $I_h = 5.8598 \times 10^{-4}\,\text{kgm}^2$ is considered.

III. MODELLING OF THE FLEXIBLE MANIPULATOR

This section provides a brief description of the modelling of the flexible robot manipulator system, as a basis of a simulation environment for development and assessment of the input shaping control techniques. The finite element method with 10 elements is considered in characterising the dynamic behaviour of the manipulator incorporating structural damping and hub inertia. Further details of the description and derivation of the dynamic model of the system can be found in Martins et al.[1] The dynamic model has also been validated with experimental exercises where a close agreement between both theoretical and experimental results has been achieved.

For a small angular displacement $\theta(t)$ and a small elastic deflection $w(x,t)$, the total displacement $y(x,t)$ of a point along the manipulator at a distance x from the hub can be described as a function of both the rigid body motion and elastic deflection measured from the line OX as

$$y(x,t) = x\theta(t) + w(x,t)$$

Using the standard Finite Element method to solve the dynamic problems, i.e. the kinetic and potential energies of an element, the element mass matrix, M_n and stiffness matrix K_n are obtained as

$$M_n = \frac{\rho A l}{420}\begin{bmatrix} m_{11} & m_{12} & m_{13} & m_{14} & m_{15} \\ m_{21} & 156 & 22l & 54 & -13l \\ m_{31} & 22l & 4l^2 & 13l & -3l^2 \\ m_{41} & 54 & 13l & 156 & -22l \\ m_{51} & -13l & -3l^2 & -22l & 4l^2 \end{bmatrix};$$

$$K_n = \frac{EI}{l^3}\begin{bmatrix} 0 & 0 & 0 & 0 & 0 \\ 0 & 12 & 6l & -12 & 6l \\ 0 & 6l & 4l^2 & -6l & 2l^2 \\ 0 & -12 & -6l & 12 & -6l \\ 0 & 6l & 2l^2 & -6l & 4l^2 \end{bmatrix}$$

where

$$\begin{aligned} m_{11} &= 140l^2(3n^2 - 3n + 1) \\ m_{12} &= m_{21} = 21l(10n - 7) \\ m_{13} &= m_{31} = 7l^2(5n - 3) \\ m_{14} &= m_{41} = 21l(10n - 3) \\ m_{15} &= m_{51} = -7l^2(5n - 2) \end{aligned}$$

l is the elemental length of the manipulator and n is number of elements.

Assembling the element mass and stiffness matrices and utilising the Lagrange equation of motion, the dynamic equation of motion of the flexible manipulator system can be obtained as

$$M\ddot{Q}(t) + D\dot{Q}(t) + KQ(t) = F(t) \tag{1}$$

where M, D and K are global mass, damping and stiffness matrices of the manipulator respectively. The damping matrix is obtained by assuming the manipulator exhibits the characteristic of Rayleigh damping. $F(t)$ is a vector of external forces and $Q(t)$ is a nodal displacement vector given as

$$Q(t) = [\theta \quad w_0 \quad \theta_0 \quad \ldots \quad w_n \quad \theta_n]^T$$

where $w_n(t)$ and $\theta_n(t)$ are the flexural and angular deflections at the end point of the manipulator respectively. In this work, the manipulator is considered as a clamped-free arm with the applied τ at the hub, the flexural and angular deflections, velocity and acceleration are all zero at the hub when $t = 0$ and the external force is $F(t) = [\tau\ 0 \ldots 0]^T$.

IV. INPUT SHAPING CONTROL SCHEME

Input shaping is a feed-forward control technique that involves convolving a desired command with a sequence of impulses known as input shaper.[5] The shaped command that results from the convolution is then used to drive the system. Design objectives are to determine the amplitude and time locations of the impulses, so that the shaped command reduces the detrimental effects of system flexibility. These parameters are obtained from the natural frequencies and damping ratios of the system. Thus, vibration reduction of a flexible manipulator system can be achieved with the input shaping technique. The input shaping process is illustrated in Figure 2. Several techniques have been investigated to obtain an efficient input shaper for a particular system. A brief description and derivation of the control technique is presented in this section.

Generally, a vibratory system of any order can be modelled as a superposition of second order systems each with a

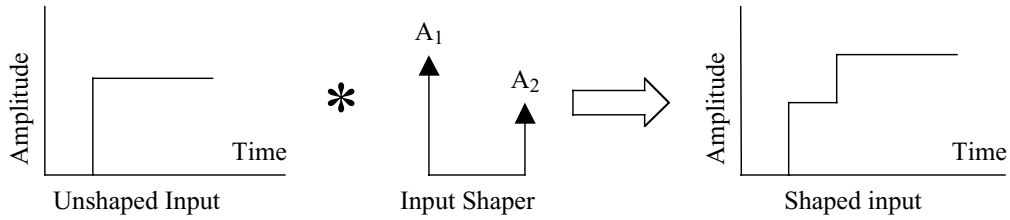

Fig. 2. Illustration of input shaping technique.

https://doi.org/10.1017/S0263574705002511 Published online by Cambridge University Press

transfer function

$$G(s) = \frac{\omega^2}{s^2 + 2\zeta\omega s + \omega^2}$$

where ω is the natural frequency of the vibratory system and ζ is the damping ratio of the system. Thus, the response of the system in the time domain can be obtained as

$$y(t) = \frac{A\omega}{\sqrt{1-\zeta^2}} e^{-\zeta\omega(t-t_0)} \sin(\omega\sqrt{1-\zeta^2}(t-t_0))$$

where A and t_0 are the amplitude and the time location of the impulse respectively. The response to a sequence of impulses can be obtained by superposition of the impulse responses. Thus, for N impulses, with $\omega_d = \omega(\sqrt{1-\zeta^2})$, the impulse response can be expressed as

$$y(t) = M \sin(\omega_d t + \beta)$$

where

$$M = \sqrt{\left(\sum_{i=1}^{N} B_i \cos\phi_i\right)^2 + \left(\sum_{i=1}^{N} B_i \sin\phi_i\right)^2},$$

$$B_i = \frac{A_i\omega}{\sqrt{1-\zeta^2}} e^{-\zeta\omega(t-t_0)}, \quad \phi_i = \omega_d t_i$$

and A_i and t_i are the amplitudes and time locations of the impulses.

The residual single mode vibration amplitude of the impulse response is obtained at the time of the last impulse, t_N as

$$V = \sqrt{V_1^2 + V_2^2} \tag{2}$$

where

$$V_1 = \sum_{i=1}^{N} \frac{A_i\omega_n}{\sqrt{1-\zeta^2}} e^{-\zeta\omega_n(t_N - t_i)} \cos(\omega_d t_i);$$

$$V_2 = \sum_{i=1}^{N} \frac{A_i\omega_n}{\sqrt{1-\zeta^2}} e^{-\zeta\omega_n(t_N - t_i)} \sin(\omega_d t_i)$$

To achieve zero vibration after the last impulse, it is required that both V_1 and V_2 in Equation (2) are independently zero. This is known as the zero vibration constraint. In order to ensure that the shaped command input produces the same rigid body motion as the unshaped reference command, it is required that the sum of amplitudes of the impulses is unity. This yields the unity amplitude summation constraint as

$$\sum_{i=1}^{N} A_i = 1 \tag{3}$$

In order to avoid response delay, time optimality constraint is utilised. The first impulse is selected at time $t_1 = 0$ and the last impulse must be at the minimum, i.e. min (t_N) The robustness of the input shaper to errors in natural frequencies of the system can be increased by taking the derivatives of V_1 and V_2 to zero. Setting the derivatives to zero is equivalent to producing small changes in vibration corresponding to the frequency changes. The level of robustness can further be increased by increasing the order of derivatives of V_1 and V_2 and set them to zero. Thus, the robustness constraints can be obtained as

$$\frac{d^i V_1}{d\omega_n^i} = 0; \quad \frac{d^i V_2}{d\omega_n^i} = 0 \tag{4}$$

Both the positive and SNA input shapers are designed by considering the constraints equations. The following section will further discuss the design of the positive and SNA input shapers.

IV.1. Positive input shaper

The requirement of positive amplitudes for the input shapers has been used in most input shaping schemes. The requirement of positive amplitude for the impulses is to avoid the problem of large amplitude impulses. For the case of positive amplitudes, each individual impulse must be less than one to satisfy the unity magnitude constraint.

The positive ZV input shaper, i.e. two-impulse sequence is designed by taking into consideration the zero residual vibration constraints, time optimality constraints and unity magnitude constraints. Hence, by setting V_1 and V_2 in Equation (2) to zero, $\sum_{i=1}^{N} A_i = 1$, $t_1 = 0$ to avoid response delay and solving yields a two-impulse sequence with parameters as

$$t_1 = 0, \quad t_2 = \frac{\pi}{\omega_d}, \quad A_1 = \frac{1}{1+K}, \quad A_2 = \frac{K}{1+K} \tag{5}$$

where

$$K = e^{-\zeta\pi/\sqrt{1-\zeta^2}}, \quad \omega_d = \omega_n\sqrt{1-\zeta^2}$$

The positive ZV shaper does not consider the robustness constraints. To increase the robustness of the positive input shaper, the robustness constraints must be considered in solving for the time locations and amplitudes of the impulses sequence. The robustness constraints equations can be obtained by setting the derivatives of V_1 and V_2 in Equation (2) to zero. By solving the zero-residual vibration, robustness, unity magnitude and time optimality constraints yield a three-impulse sequence known as the positive ZVD shaper.

To obtain a positive input shaper with higher level of robustness, another set of constraint equation, i.e. by setting the second derivatives of V_1 and V_2 in Equation (2) to zero must be considered in solving for the amplitudes and time locations of the impulse sequence. Simplifying $d^2V_i/d\omega_n^2$, yields

$$\frac{d^2V_1}{d\omega_n^2} = \sum_{i=1}^{N} A_i t_i^2 e^{-\zeta\omega_n(t_N - t_i)} \sin(\omega_d t_i);$$

$$\frac{d^2V_2}{d\omega_n^2} = \sum_{i=1}^{N} A_i t_i^2 e^{-\zeta\omega_n(t_N - t_i)} \cos(\omega_d t_i) \tag{6}$$

The positive ZVDD input shaper, i.e. four-impulse sequence is obtained by setting Equations (2) and (6) to

https://doi.org/10.1017/S0263574705002511 Published online by Cambridge University Press

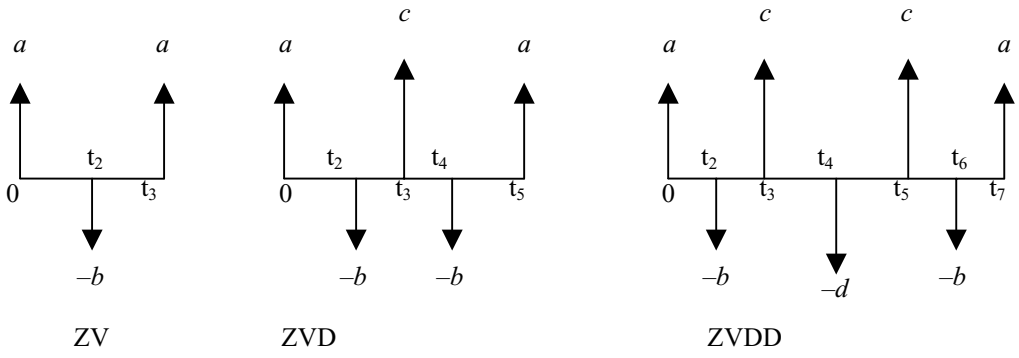

Fig. 3. SNA shaper.

zero and solving with the other constraint equations. Hence, a four-impulse sequence can be obtained with the parameters as

$$t_1 = 0, \quad t_2 = \frac{\pi}{\omega_d}, \quad t_3 = \frac{2\pi}{\omega_d}, \quad t_4 = \frac{3\pi}{\omega_d}$$

$$A_1 = \frac{1}{1+3K+3K^2+K^3}, \quad A_2 = \frac{3K}{1+3K+3K^2+K^3} \tag{7}$$

$$A_3 = \frac{3K^2}{1+3K+3K^2+K^3}, \quad A_4 = \frac{K^3}{1+3K+3K^2+K^3}$$

where K as is equation (5).

Note that the positive ZVDD shaper is triple the duration of the ZV shaper. Theoretically, speed of a shaped command reduces by the duration of the shaper. Therefore, the speed of ZVDD response is the slowest as compared to other input shapers. In order to handle higher vibration modes, an impulse sequence for each vibration mode can be designed independently. Then, the impulse sequences can be convoluted together to form a sequence of impulses that attenuate vibration at higher modes.

IV.2. Specified Negative Amplitude (SNA) input shapers

Input shaping techniques based on positive input shaper has been proved to be able to reduce vibration of a system. In order to achieve higher robustness, the duration of the shaper is increased and thus, increases the delay in the system response. By allowing the shaper to contain negative impulses, the shaper duration can be shortened, while satisfying the same robustness constraint.

To include negative impulses in a shaper requires the impulse amplitudes to switch between 1 and −1 as

$$A_i = (-1)^{i+1}; \quad i = 1, \ldots, \mathrm{n} \tag{8}$$

The constraint in Equation (8) yields useful shapers as they can be used with a wide variety of inputs without leading to over-currenting. For a UM negative ZV shaper, i.e. the magnitude of each impulse is |1|, the shaper duration is one-third of the vibration period of an undamped system, while the shaper duration for the positive shaper is half of the vibration period. However, the increase in the speed of system response achieved using the negative impulse is at the expense of some tradeoffs and penalties. The shapers containing negative impulses have tendency to excite unmodeled high modes and they are slightly less robust as compared to the positive shapers. Besides, negative input shapers require more actuator effort than the positive shapers due to high changes in the set-point command at each new impulse time location.

To overcome the disadvantages, an SNA input shaper is introduced, whose negative amplitudes can be set to any value. To design the SNA input shapers, the constraint equations described in the previous section must be considered. Figure 3 shows the exact form of the SNA input shaper. Further, to design an SNA-ZV input shaper, the zero residual vibration constraints and unity amplitude summation constraints in Equations (2) and (3) are considered respectively. Moreover, by considering the form of SNA shaper shown in Figure 3, the unity amplitude summation constraints equation can be obtained as

$$2a - b = 1 \tag{9}$$

The values of a and b can be set to any value that satisfy the constraint in Equation (9). However, the suggested values of a and b are less than |1| to avoid the increase of the actuator effort. Subsequently, the time locations, t_2 and t_3 can be determined by solving the time-optimality constraint.

For SNA-ZVD and SNA-ZVDD input shapers, the same technique is applied to determine the time locations of the impulses. However, the robustness constraint equations are considered depending on the level of robustness required for both SNA-ZVD and SNA-ZVDD input shapers.

V. IMPLEMENTATION AND RESULTS

The positive and SNA input shapers are designed based on the vibration frequencies and damping ratios of the flexible manipulator system. Previous experimental results with the flexible manipulator experimental rig have shown that the damping ratios of the system are 0.026, 0.038 and 0.4 for the first, second and third modes respectively.[16] The natural frequencies were obtained by exciting the flexible manipulator with an unshaped bang-bang torque. The input shapers were designed for pre-processing the bang-bang torque input and applied to the system in an open-loop configuration, as shown in Figure 4. In this work, the unshaped and the shaped inputs were designed with a sampling frequency of 2 kHz.

https://doi.org/10.1017/S0263574705002511 Published online by Cambridge University Press

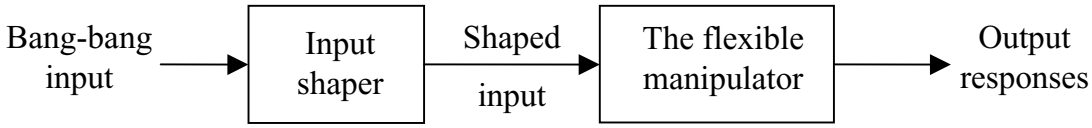

Fig. 4. Block diagram of input shaping control configuration.

Simulation results of the response of the flexible manipulator to the unshaped input, shaped inputs with positive and negative input shapers are presented in this section in the time and frequency domains. To investigate the performance of both the positive and negative input shapers, the results are examined in comparison to the unshaped bang-bang torque input for a similar input level in each case. Three system responses namely the hub-angle, hub-angular velocity and end-point acceleration are obtained. Moreover, the power spectral density (PSD) of the end-point acceleration is evaluated to investigate the dynamic behaviour of the system in the frequency domain. Three criteria are used to evaluate the performances of the control schemes:

(1) Level of vibration reduction at the natural frequencies. This is accomplished by comparing the responses to the shaped inputs with the response to the unshaped input.
(2) The time response specifications. Parameters that are evaluated are rise time, settling time and overshoot of the hub-angle response. The settling time is calculated on the basis of $\pm 2\%$ of the steady-state value. Moreover, the magnitude of oscillation of the system response is observed.
(3) Robustness to parameter uncertainty. To examine the robustness of the techniques, the system performance is assessed with 30% error tolerance in natural frequencies. This is incorporated in the design of the input shapers.

V.1. Unshaped bang-bang torque input

In this work, the unshaped bang-bang torque input of amplitude ± 0.3 Nm is used as the reference command. Figure 5 shows the single-switch bang-bang torque used as the input to the system and its corresponding PSD. The input is applied at the hub of the flexible manipulator. The bang-bang torque is required to have positive and negative period to allow the manipulator to, initially, accelerate and then decelerate and eventually, stop at the target position. The first three modes of vibration of the system are considered, as these dominate the dynamics of the system.

Figure 6 shows the responses of the flexible manipulator system to the unshaped bang-bang torque input in time-domain and frequency domain (PSD). These results were considered as the system response to the unshaped input and will be used to evaluate the performance of the input shaping techniques. The hub-angle, hub-velocity and end-point acceleration responses show that a significant vibration occurs during the movement of the flexible manipulator. The steady-state hub-angle of 38° for the flexible manipulator system was achieved within the rise and settling times of 0.387 s and 0.7875 s, respectively. The hub-velocity response shows oscillation between -50 and 200 degree/sec, whereas the end-point acceleration response was found to oscillate between ± 300 m/s^2. Resonance frequencies of the system were obtained by transforming the time-domain representation of the system responses into frequency domain using power spectral analysis. The vibration frequencies of the flexible manipulator system were obtained as 12, 35 and 65 Hz for the first three modes as demonstrated in Figure 6.

V.2. Positive input shaper

Positive ZV shaper (two-impulse sequence) and positive ZVDD (four-impulse sequence) were designed for three modes utilising the properties of the system. With the exact natural frequencies of 12, 35 and 65 Hz, the time locations and amplitudes of the impulses were obtained by solving equations (5) and (7). For evaluation of robustness, input shapers with error in natural frequencies were also evaluated.

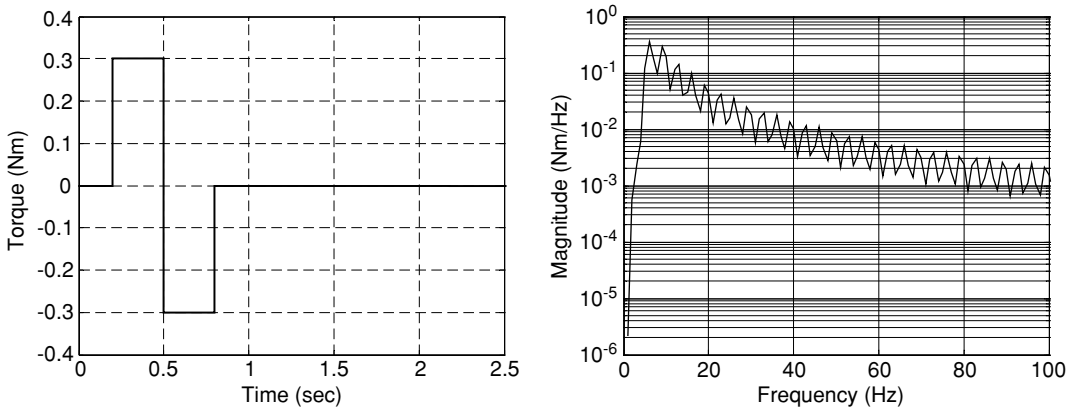

(a) Time domain (b) PSD

Fig. 5. The unshaped bang-bang torque input.

https://doi.org/10.1017/S0263574705002511 Published online by Cambridge University Press

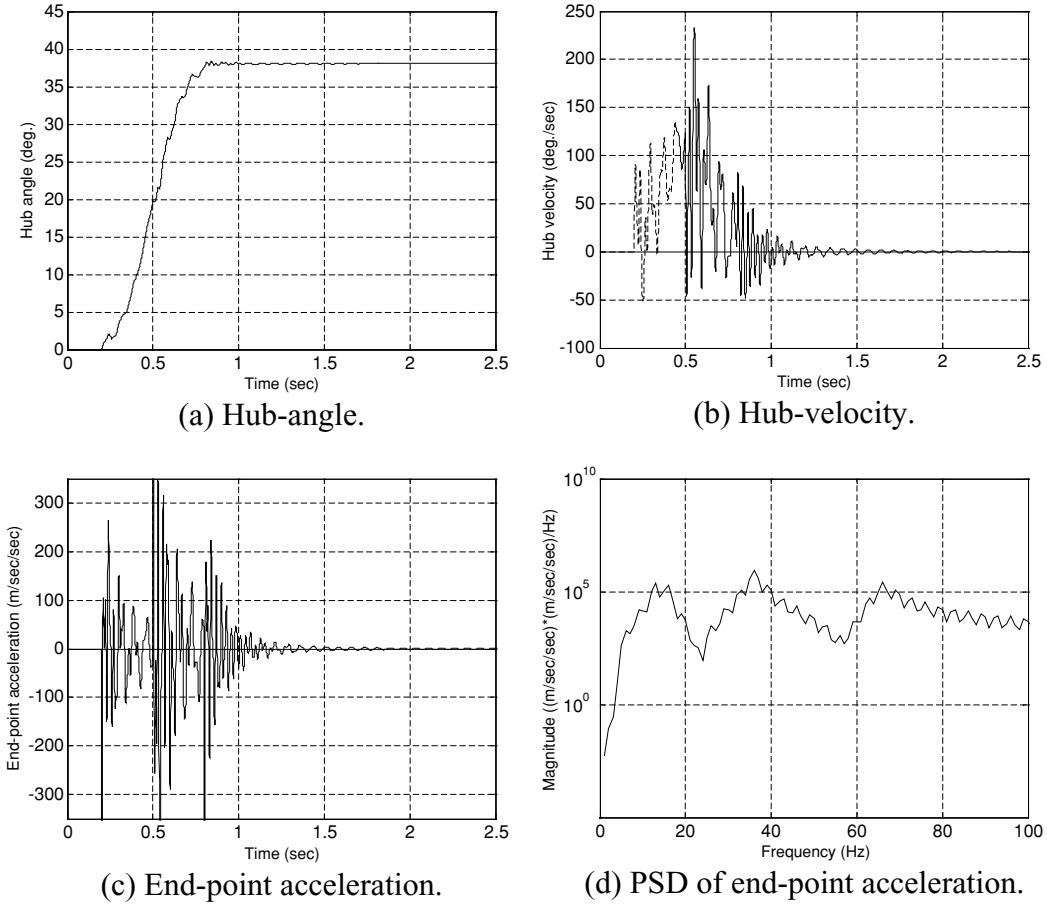

(a) Hub-angle. (b) Hub-velocity.

(c) End-point acceleration. (d) PSD of end-point acceleration.

Fig. 6. Response of the flexible manipulator to the unshaped bang-bang torque input.

With the 30% error in natural frequency, the system vibrations were considered at 15.6, 45.5 and 84.5 Hz for the three modes of vibration. Similarly, the amplitudes and time locations of the input shapers with 30% erroneous natural frequencies for both the positive ZV and ZVDD input shapers were calculated. For digital implementation of the input shapers, locations of the impulses were selected at the nearest sampling time. The shaped inputs using both positive ZV and ZVDD shapers with exact natural frequency and their corresponding PSDs are shown in Figure 7. It can be noticed from Figure 7(a) that with higher number of impulses, the shaped input is slower. Besides, the magnitudes of the PSD at the natural frequencies were reduced as the number of impulses increased.

The system responses of the flexible manipulator to the shaped bang-bang torque input with exact natural frequencies using the positive shapers are shown in Figure 8. It is noted that the vibration in the hub-angle, hub-velocity and end-point acceleration responses were significantly reduced. Table I summarises the levels of vibration reduction of the

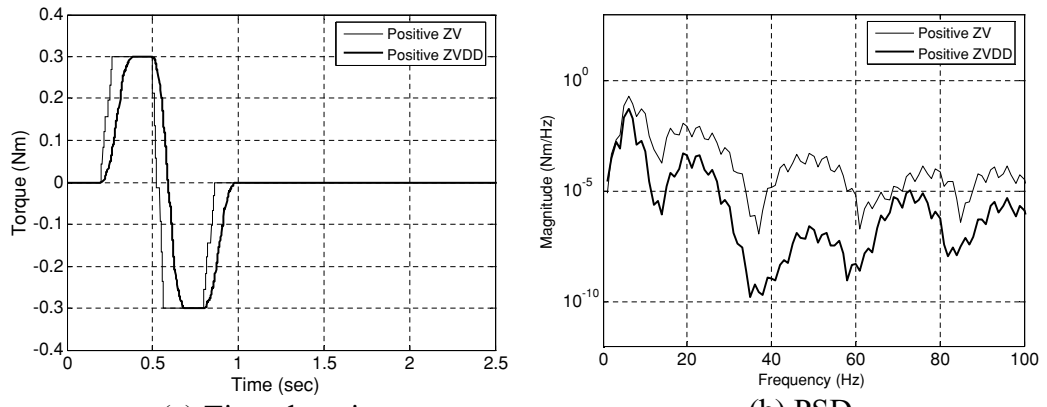

(a) Time domain. (b) PSD.

Fig. 7. Shaped bang-bang torque with positive ZV and ZVDD shapers.

https://doi.org/10.1017/S0263574705002511 Published online by Cambridge University Press

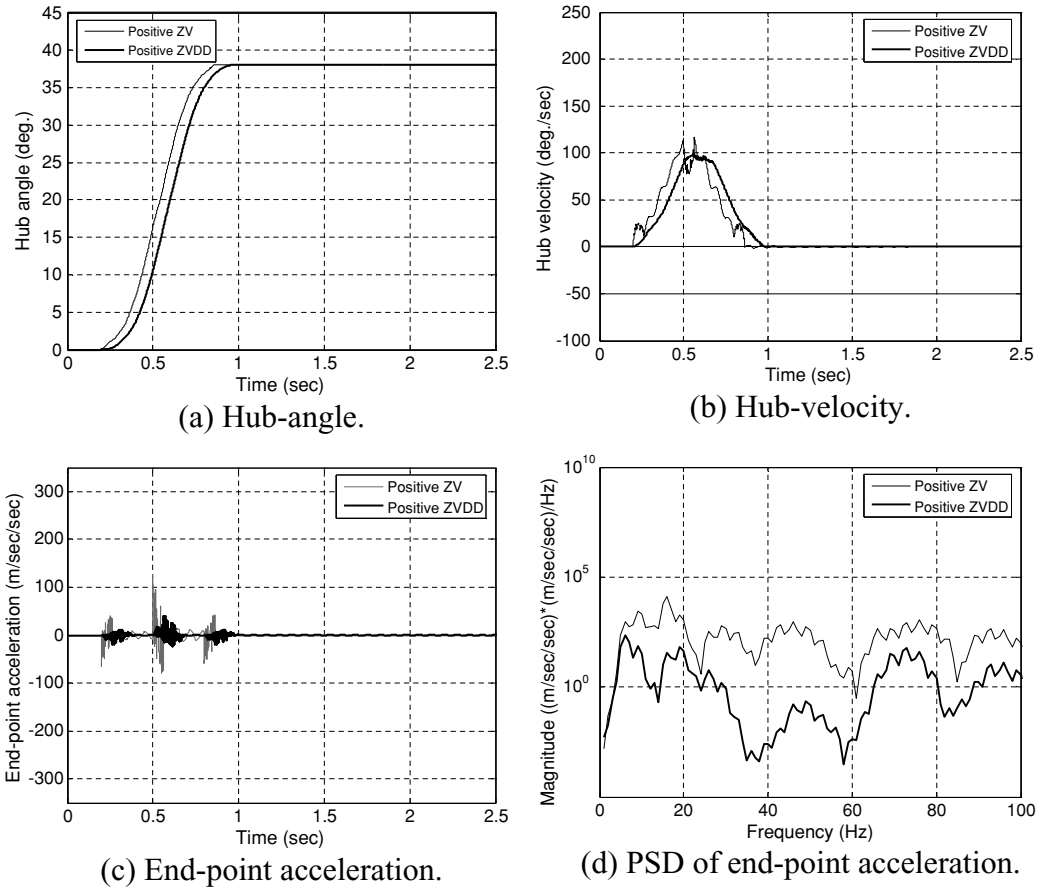

Fig. 8. Response of the flexible manipulator with exact natural frequencies using the positive shapers.

system responses at the first three modes in comparison to the unshaped bang-bang torque input. Higher levels of vibration reduction were obtained with positive ZVDD as compared to the shaped input with positive ZV. However, with positive ZVDD shaper, the system response is slower. Hence, it is evident that the speed of the system response reduces with the increase in the number of impulses. The corresponding rise time, setting time and overshoot of the hub-angle response using the positive ZV and ZVDD shapers with exact natural frequencies is depicted in Table I. It is noted that a much faster hub-angle response with less overshoot, as compared to the unshaped input, was achieved.

To examine the robustness of the positive shapers, the positive shapers with 30% error in vibration frequencies were designed and applied to the flexible manipulator system. Figure 9 shows the response of the manipulator to the shaped input using positive ZV and ZVDD shapers with erroneous natural frequencies. The vibration of the system were considerable reduced as compared to the system with unshaped input (Figure 7). However, the level of vibration reduction is slightly less than the case with exact natural frequencies. Table I summarises the levels of vibration reduction with erroneous natural frequencies in comparison to the unshaped input. The time response specifications of the hub-angle with error in natural frequencies are summarised in Table I. It is noted that the response is slightly faster for the shaped input with error in natural frequencies than the case with exact frequencies. However, the overshoot of the response is slightly higher than the case with exact frequencies. Significant vibration reduction was achieved in the overall response of the system to the shaped input

Table I. Level of vibration reduction with the end-point acceleration and specifications of hub-angle response using positive shapers.

		Reduction (dB) of vibration at the end-point			Specifications of hub-angle response		
Frequency	Type of shaper	Mode 1	Mode 2	Mode 3	Rise time (s)	Settling time (s)	Overshoot (%)
Exact	ZV	45.93	80.89	55.55	0.3695	0.8220	0.045
	ZVDD	93.26	151.26	81.74	0.3810	0.8845	0.002
Error	ZV	17.98	22.89	27.81	0.3750	0.8140	0.240
	ZVDD	53.05	68.36	82.85	0.3760	0.8160	0.008

https://doi.org/10.1017/S0263574705002511 Published online by Cambridge University Press

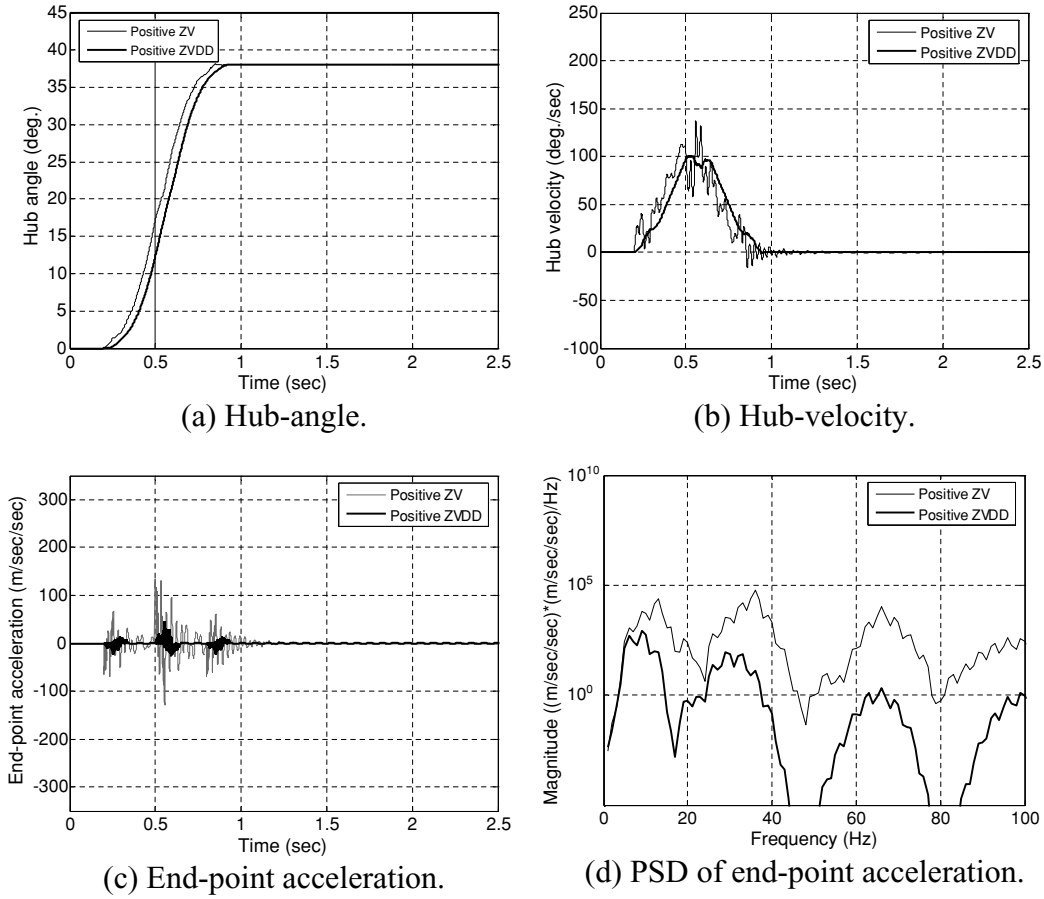

Fig. 9. Response of the flexible manipulator with 30% error in natural frequencies using the positive shapers.

with 30% error in natural frequencies, and hence proved the robustness of the positive shapers.

V.3. SNA shapers

The form of the shaper shown in Figure 3 is considered in designing the SNA shaper. The amplitudes of the SNA shaper were deduced as [0.7 −0.4 0.7] and [0.3 −0.2 0.5 −0.2 0.5 −0.2 0.3] for the SNA-ZV and SNA-ZVDD shapers, respectively. The time locations of the impulses were obtained by solving the constraint equation. However, as the constant equations are highly non-linear and cannot be simplified, in this work, an optimisation technique based on least square error was utilised. Similar to the positive shapers, the SNA shapers were designed for the first three modes of vibration with exact natural frequencies i.e. 12, 35, 65 Hz and the same damping ratios. To examine the robustness of the SNA shapers, the system vibrations were considered at 30% error in natural frequencies, i.e. 15.6, 45.5 and 84.5 Hz. Similarly, the time locations of the shapers were obtained by solving the constraint equations.

Figure 10 shows the shaped inputs using the SNA-ZV and SNA-ZVDD shapers and their corresponding PSDs. It is noted that the shaped bang-bang torque inputs with the SNA shapers are not as smooth as compared to the positive shapers. This is due to higher number of switching of the actuator. As in the case of a positive shaper, the shaped input with SNA-ZVDD shaper is delayed more than the shaped input with SNA-ZV shaper. Similarly, the magnitudes of he PSD were reduced as the number of impulses increased.

The system responses of the flexible manipulator with the SNA-ZV and SNA-ZVDD shapers are shown in Figure 11. It is noted that the overall system vibrations were significantly reduced with the shaped input even though the level of vibration reduction was less than the case with the positive shapers. The levels of vibration reduction with the end-point acceleration at the first three modes in comparison to the unshaped bang-bang torque input and the time-response specification of the hub-angle response are summarised in Table II. It is noted that the levels of vibration reduction increase with increasing number of impulses of the SNA shapers. The result demonstrates that the response with negative shaper is faster than the case with positive shapers. However, the responses are slower as compared to the unshaped input.

To investigate the robustness of the SNA shapers, the shapers were designed with 30% error in natural frequencies for the first three modes. The responses of the flexible manipulator to the shaped bang-bang torque input with 30% error in natural frequencies using the SNA shapers are shown in Figure 12. The vibrations in the system responses were considerably reduced although not as much as the case with exact natural frequencies. The levels of vibration reduction in comparison to the unshaped input and the specifications of hub-angle response with erroneous natural frequencies are summarised in Table II. It is noted that the response is slightly

https://doi.org/10.1017/S0263574705002511 Published online by Cambridge University Press

Table II. Level of vibration reduction with the end-point acceleration and specifications of hub-angle response using SNA shapers.

		Reduction (dB) of vibration at the end-point			Specifications of hub-angle response		
Frequency	Type of shaper	Mode 1	Mode 2	Mode 3	Rise time (s)	Settling time (s)	Overshoot (%)
Exact	ZV	45.18	41.99	45.64	0.3685	0.8155	0.063
	ZVDD	80.96	140.92	74.80	0.3810	0.8750	0.003
Error	ZV	16.85	11.57	40.27	0.3750	0.8110	0.410
	ZVDD	50.82	53.99	90.03	0.3750	0.8540	0.015

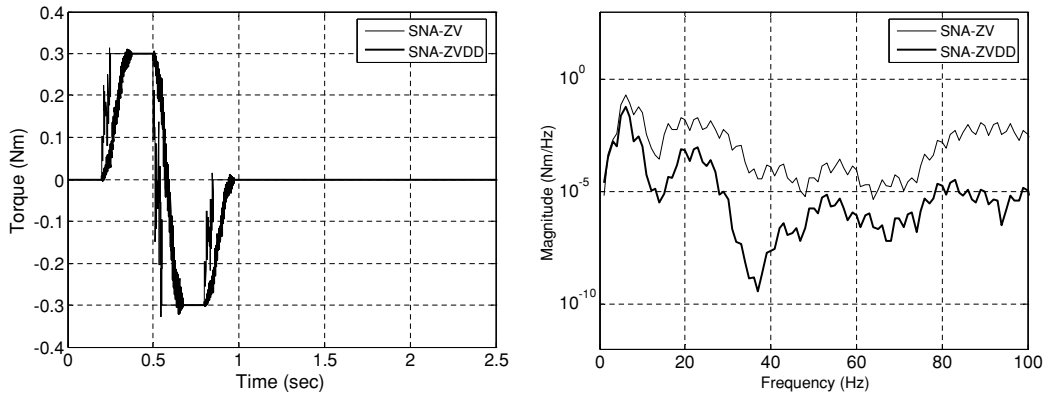

(a) Time domain. (b) PSD.

Fig. 10. Shaped bang-bang torque with SNA-ZV and ZVDD shapers.

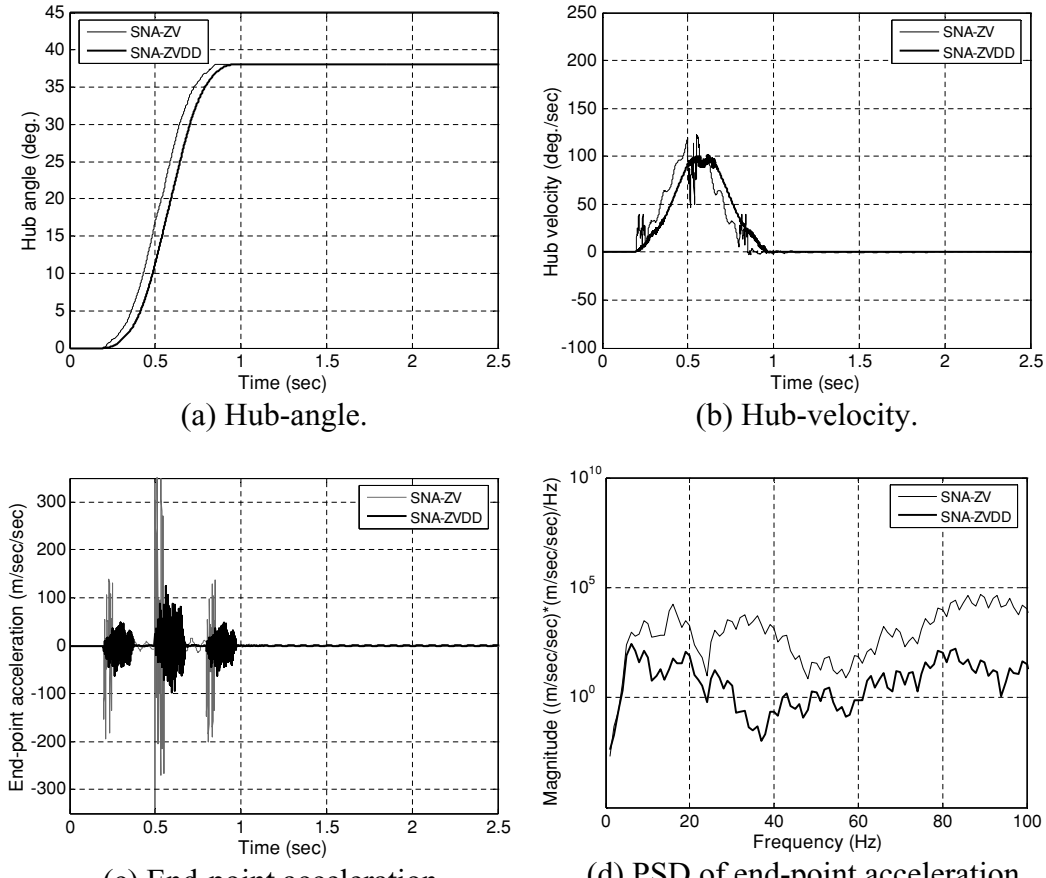

(a) Hub-angle. (b) Hub-velocity.

(c) End-point acceleration. (d) PSD of end-point acceleration.

Fig. 11. Response of the flexible manipulator with exact natural frequencies using SNA shapers.

https://doi.org/10.1017/S0263574705002511 Published online by Cambridge University Press

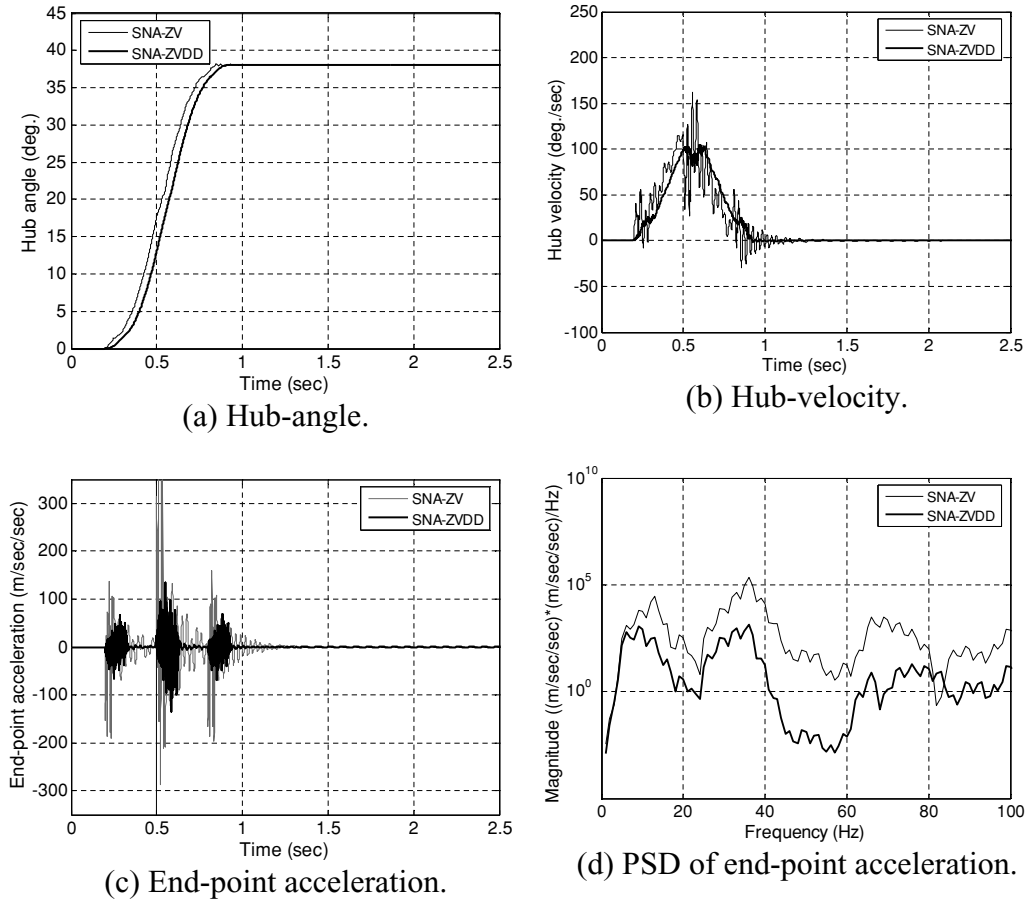

Fig. 12. Response of the flexible manipulator with 30% error in natural frequencies using SNA shapers.

faster than the case with exact natural frequencies. Despite the increase of overshoot as compared to the case with exact frequencies, the overshoot of the response with erroneous shaped input was reduced as compared to the response of the unshaped input.

V.4. Comparative performance assessment

By comparing the results presented in Tables I and II, it is noted that higher performance in the reduction of vibration of the system is achieved with the positive input shaping technique. This is observed and compared to the SNA input shapers at the first three modes of vibration. The performance of the positive input shaper is also evidenced in the magnitude of vibration with the hub-angle, hub-velocity and end-point acceleration responses in Figures 8 and 11. For comparative assessment, the levels of vibration reduction with the end-point acceleration using the positive and SNA shapers are shown with the bar graphs in Figure 13. The result shows that highest level of vibration reduction is achieved with the positive ZVDD shaper, followed by the SNA-ZVDD shaper, positive ZV shaper and lastly the SNA-ZV shaper. Therefore, it can be concluded that overall the positive input shapers provide better performance in vibration reduction as compared to the SNA shapers. Comparisons of the specifications of the hub-angle responses using both the positive and SNA shapers are summarised in Figure 14 for the rise and settling times. It is noted that the differences in rise times of the hub-angle response for the positive and SNA shapers are negligibly small. However, the settling time of the hub-angle response using the SNA-ZV shaper is faster than the case using the positive-ZV shaper, as well as the case with SNA-ZVDD and positive ZVDD shapers. The result reveals that the speed of the system response can be improved by using a negative impulse input shapers.

Comparison of the results shown in Tables I and II for the shaping techniques with error in natural frequencies reveals that the higher robustness to parameter uncertainty is achieved with the positive input shaping technique. For both the positive and SNA input shapers, errors in natural frequencies can successfully be handled, especially with a

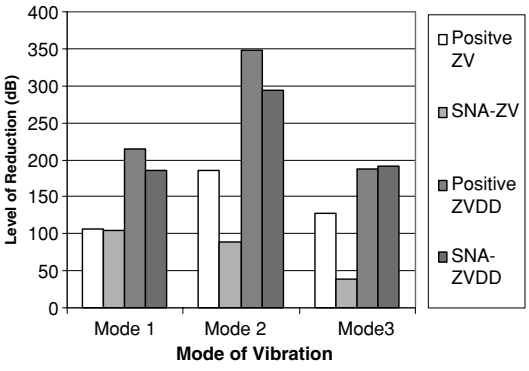

Fig. 13. Level of vibration reduction with exact natural frequencies using positive and SNA shapers.

https://doi.org/10.1017/S0263574705002511 Published online by Cambridge University Press

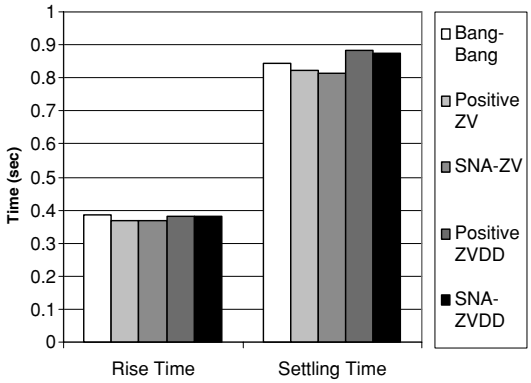

Fig. 14. Rise and settling times of the hub-angle response with exact natural frequencies using positive and SNA shapers.

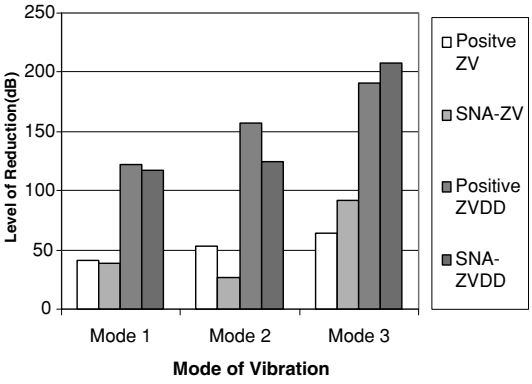

Fig. 15. Level of vibration reduction with erroneous natural frequencies using positive and SNA shapers.

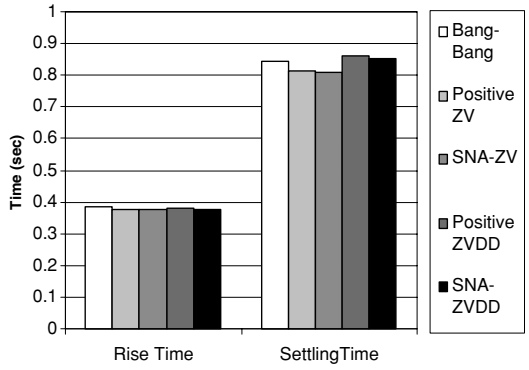

Fig. 16. Rise and settling times of the hub-angle response with erroneous natural frequencies using positive and SNA shapers.

higher number of impulses. This is revealed by comparing the magnitude of vibration of the system in Figures 9 and 12 and further evidenced in Figure 15. Comparisons of the hub-angle response with the positive and negative input shapers with erroneous natural frequencies are summarised in Figure 16. The results show a similar pattern as in the case of exact natural frequencies. The system response with SNA shaper provides slightly faster responses than the positive input shaper.

VI. CONCLUSION

Investigations into vibration control of a flexible manipulator using input shaping techniques with positive and SNA shapers have been presented. Performances of the techniques have been evaluated in terms of level of vibration reduction, time response specifications and robustness. Effects of using the positive and negative amplitudes shapers and a higher number of impulses have also been studied. A significant reduction in the system vibrations has been achieved with the input shaping techniques regardless of the polarities of the shapers. A comparison of the results has demonstrated that the input shaping using positive shapers provide higher level of vibration reduction and robustness as compared to the cases using negative (SNA) shapers. By using the negative input shapers (SNA-ZV and ZVDD), the speed of the response is slightly improved at the expense of decrease in the level of vibration reduction.

References

1. J. M. Martins, Z. Mohamed, M. O. Tokhi, J. Sá da Costa and M. A. Botto, "Approaches for dynamic modelling of flexible manipulator systems", *IEE Proceedings-Control Theory and Application* **150**(4), 401–411 (2003).
2. S. Yurkovich, "Flexibility effects on performance and control" In: *Robot Control* (Eds.: M. W. Spong, F. L. Lewis and C. T. Abdallah, IEEE Press, 1992), Part 8, pp. 321–323.
3. J. C. Swigert, "Shaped torque techniques", *Journal of Guidance and Control* **3**(5), 460–467 (1980).
4. H. Moulin and E. Bayo, "On the accuracy of end-point trajectory tracking for flexible arms by non-causal inverse dynamic solution", *Transactions of ASME: Journal of Dynamic Systems, Measurement and Control* **113**, 320–324 (1991).
5. N. C. Singer and W. P. Seering, "Preshaping command inputs to reduce system vibration", *Transactions of ASME: Journal of Dynamic Systems, Measurement and Control* **112**(1), 76–82 (1990).
6. T. Onsay and A. Akay, "Vibration reduction of a flexible arm by time optimal open-loop control", *Journal of Sound and Vibration* **147**(2), 283–300 (1991).
7. P. H. Meckl and W. P. Seering, "Experimental evaluation of shaped inputs to reduce vibration of a cartesian robot", *Transactions of ASME: Journal of Dynamic Systems, Measurement and Control* **112**(6), 159–165 (1990).
8. W. E. Singhose, N. C. Singer and W. P. Seering, "Comparison of command shaping methods for reducing residual vibration", *Proceedings of European Control Conference* Rome (1995) pp. 1126–1131.
9. M. O. Tokhi and A. K. M. Azad, "Control of flexible manipulator systems", *Proceedings of IMechE-I: Journal of Systems and Control Engineering* **210**, 283–292 (1996).
10. L. Y. Pao, "Strategies for shaping commands in the control of flexible structures", *Proceedings of Japan-USA-Vietnam Workshop on Research and Education in Systems, Computation and Control Engineering*, Vietnam (2000) pp. 309–318.
11. Z. Mohamed, J. M. Martins, M. O. Tokhi, J. Sá da Costa and M. A. Botto, "Vibration control of a very flexible manipulator system", *Control Engineering Practice* **13**(3), 267–277 (2005).
12. B. W. Rappole, N. C. Singer and W. P. Seering, "Input shaping with negative sequences for reducing vibrations in flexible structures", *Proceedings of American Control Conference*, San Francisco (1993) pp. 2695–2699.

https://doi.org/10.1017/S0263574705002511 Published online by Cambridge University Press

13. W. Singhose, "Command generation for flexible system", *Ph.D. Thesis* (*Massachusetts Institute of Technology*, 1997).
14. W. Singhose, N. C. Singer and W. P. Seering, "Design and implementation of time-optimal negative input shapers", *Proceedings of International Mechanical Engineering Congress and Exposition*, Chicago (1994) pp. 151–157.
15. W. Singhose and B. W. Mills, "Command generation using specified-negative-amplitude input shapers", *Proceedings of the American Control Conference*, San Diego, California (1999) pp. 61–65.
16. M. O. Tokhi, Z. Mohamed and M. H. Shaheed, "Dynamic characterisation of a flexible manipulator system", *Robotica* **19**, Part 5, 571–580 (2001).

https://doi.org/10.1017/S0263574705002511 Published online by Cambridge University Press